Supplementary figures

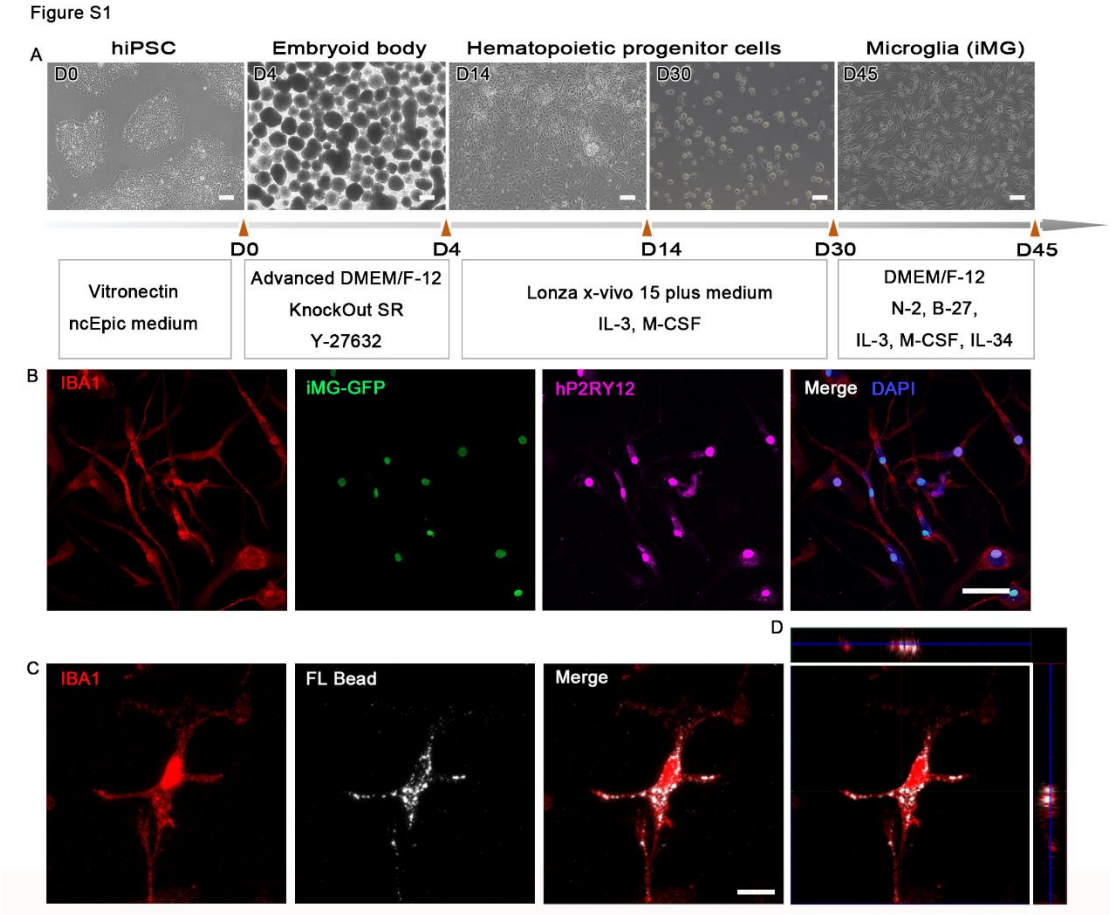

Fig. S1 Generation and characterization of human iPSC-derived microglia-like cells. (A) Schematic diagram of procedure for iMG generation and representative images at different differentiation stages. (B) Immunofluorescence images of microglial marker IBA1 and hP2RY12. (C) Phagocytosis of poly(methylmethacrylate) fluorescent nano-beads. (D) Co-localization analysis of (C). Scale bar: 100 μm (A). Scale bar: 50 μm (B). Scale bar: 10 μm (C).

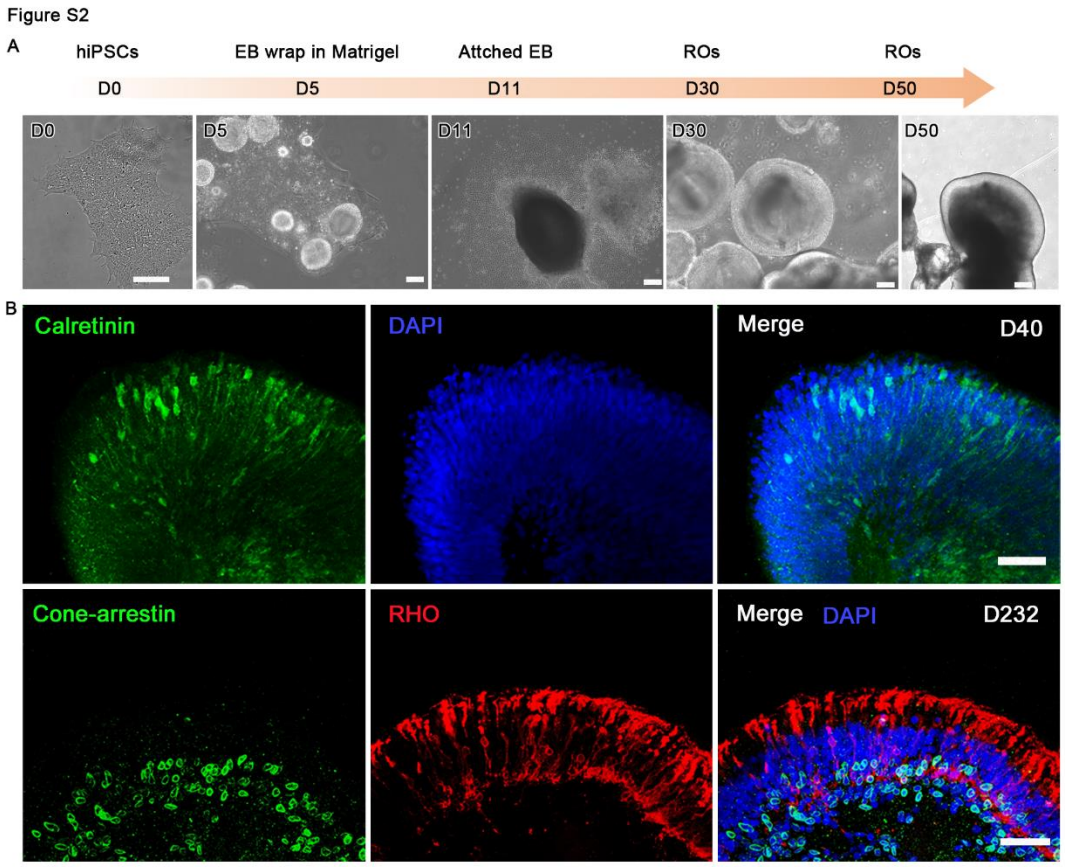

Fig. S2 Generation and characterization of retinal organoids derived from hiPSCs. (A) Schematic diagram of procedure for iMG generation and representative images at different differentiation stages. Scale bar: 100 μm. (B) Immunofluorescence images of amacrine marker Calretinin, rod photoreceptor marker rhodopsin (RHO), and cone photoreceptor marker cone-arrestin. Scale bar: 50 μm.

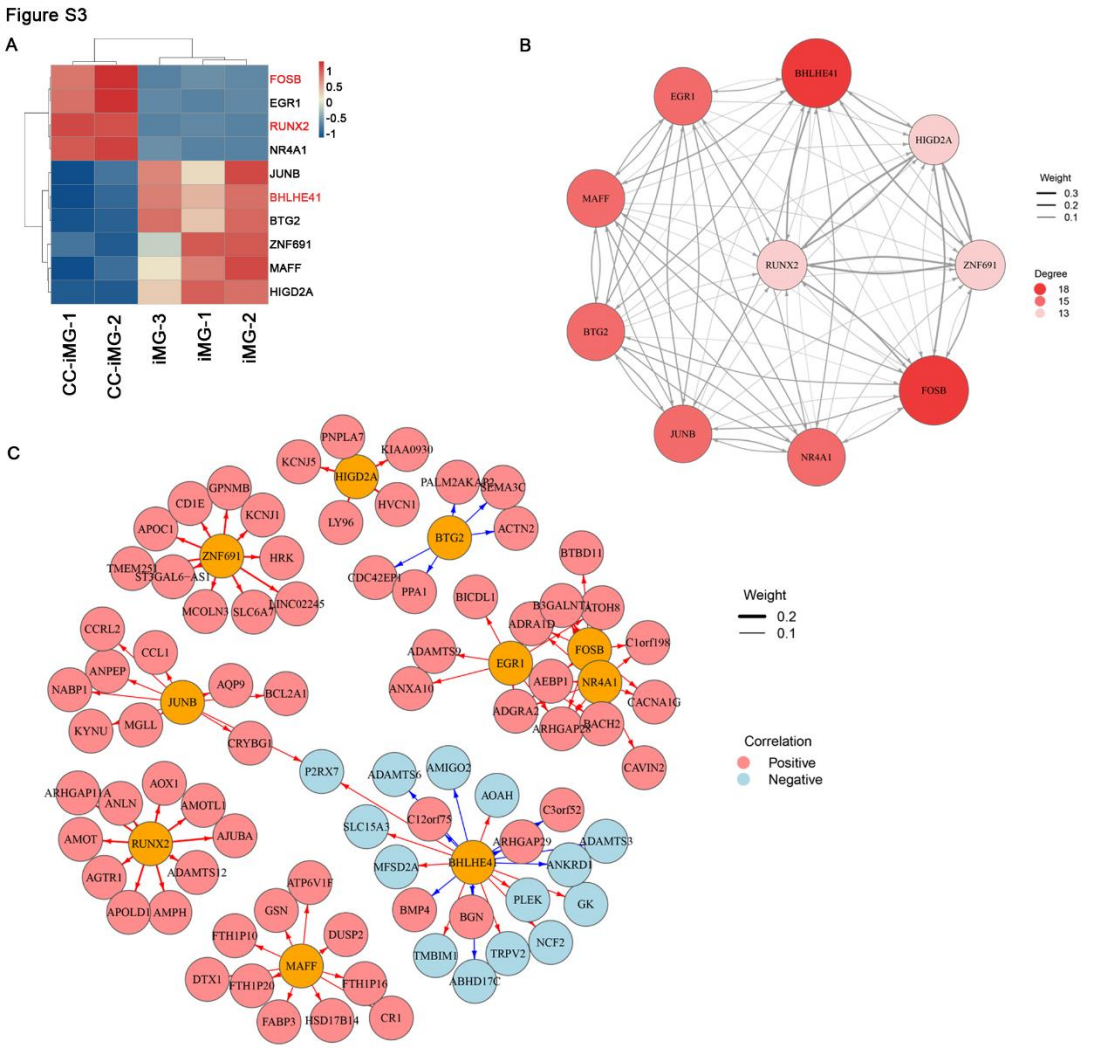

Fig. S3 Retinal cell interaction affects the expression of transcription factors in iMG. (A) Heatmap visualization of the normalized gene expression levels of transcription factors (TFs) crucial for microglial development. (B) Network of TFs differentially expressed in CC-iMG compared to iMG control. (C) From the expression and modularity analysis of target genes, we find target genes that are either downregulated (blue) or upregulated (red) in CC-iMG compared to iMG control.

Figure S4

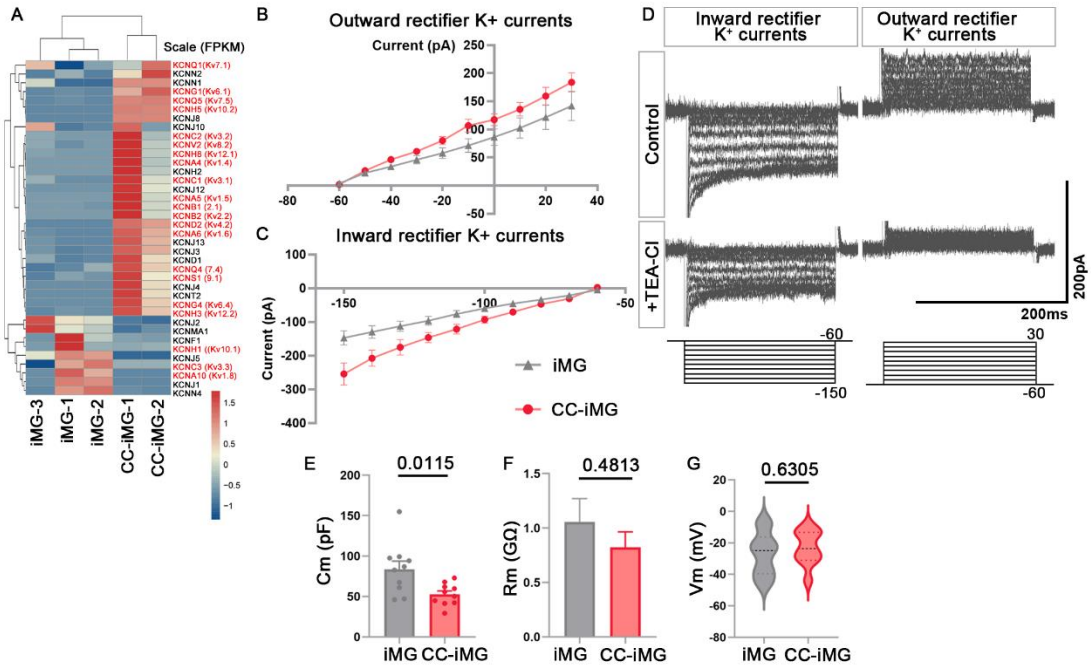

Fig. S4 Retinal cell interaction enhanced ion channel gene expression and K+ channel currents. (A) Heatmap visualization of the normalized gene expression levels demonstrating that K+ channels are significantly changed in CC-iMG. Average amplitude of outward (B) and inward (C) currents. (D) Representative images of an inward and outward rectifier K^+ current after inhibited with TEA-Cl. Data are represented as means ± SEM; n=10 cells in of iMG and CC-iMG. Related to Fig. 5. (E-G) Passive membrane properties of iMG and CC-iMG.

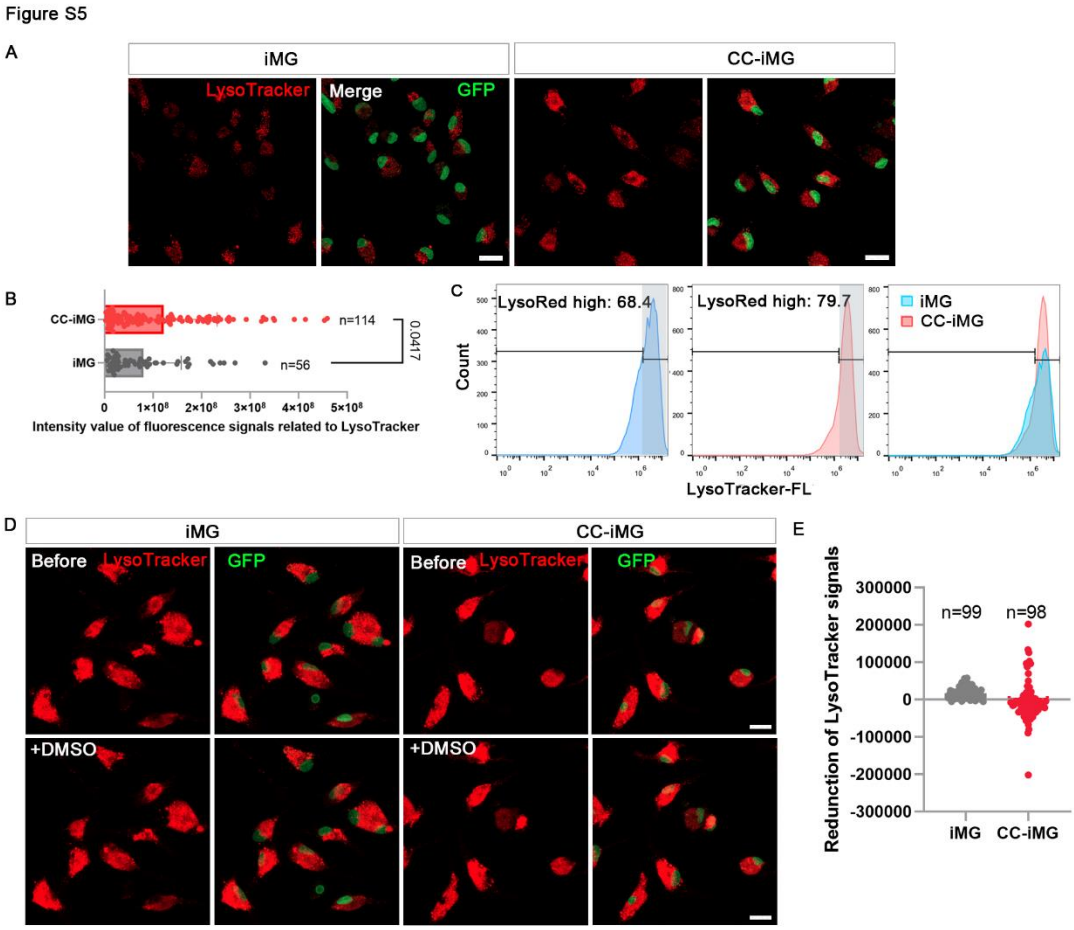

Fig.S5 Co-culture with retinal organoids promotes organelle maturation in iMG. (A) Representative images of LysoTracker red staining of iMG and CC-iMG. (B) Quantification of intensity of cell area stained by LysoTracker. (C) Flow cytometry analysis of LysoTracker stained iMG and CC-iMG. (C) Representative images of LysoTracker red staining of iMG and CC-iMG before and after adding vehicle (DMSO). (D) Quantification of reduced fluorescent intensity of LysoTracker after DMSO treatment. The mean value was used as background noise. (B, E) Data are represented as means ± SD. Scale bar: 20 μm (A, D). Related to Fig. 7.

Figure S6

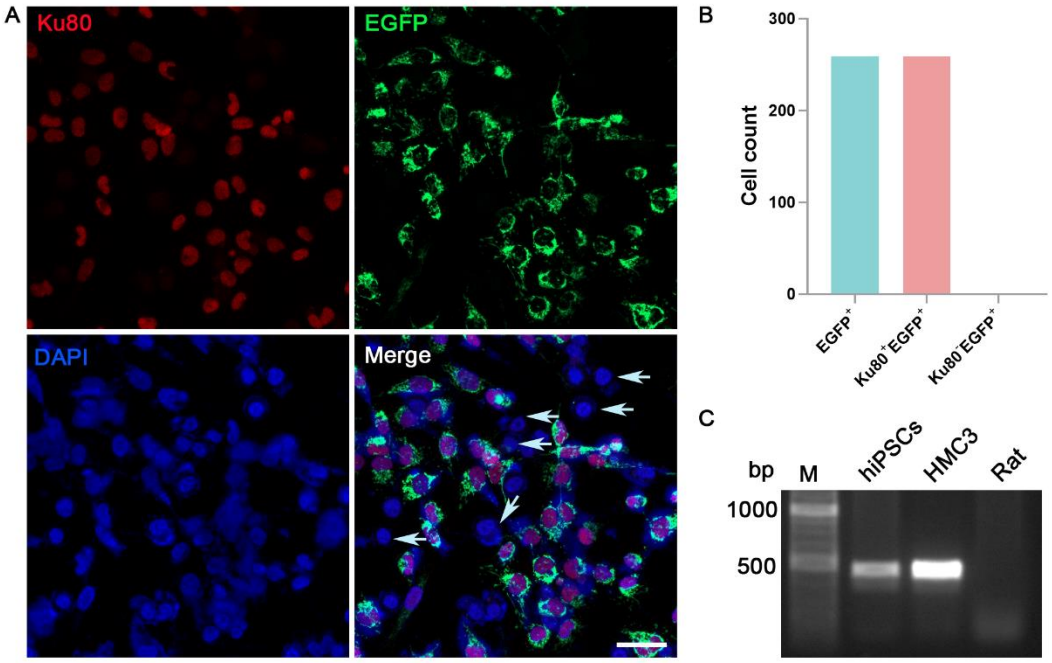

Fig. S6 Confirmation of human origin of HMC3. (A) Representative images of anti-Ku80, a human nuclear marker, immunostaining in HMC3 and BV2 cells, a murine microglial cell line. HMC3 cells were labeled with EGFP expressed specifically in mitochondria. Scale bar: 50 μm. (B) Statistic analysis of Ku80 positive rate in $EGFP^+$ HMC3 showing 100% HMC3 cells are human cells. Data are derived from 259 from 6 images. (C) PCR amplification of human CYCT1-specific primers. Genomic DNA from hiPSCs, HMC3, and rat tissue was used as the template.